Spectrochimica Acta Part A: Molecular and Biomolecular Spectroscopy 126 (2014) 242–253

Contents lists available at ScienceDirect

Spectrochimica Acta Part A: Molecular and Biomolecular Spectroscopy

journal homepage: www.elsevier.com/locate/saa

Morphological and pharmacological investigation on some biopotent materials derived from substituted pyrimidine and imidazole enzyme constituents

Sutha Shobana [a], Perumal Subramaniam [b,*], Jeyapraksh Dharmaraja [c], Arvind Narayan [d]

[a] Department of Chemistry, Division of Science and Humanities, Rajas International Institute of Technology for Women, Ozhuginaserri, Nagercoil 629 001, Tamil Nadu, India
[b] Department of Chemistry and Research Centre, Aditanar College of Arts and Science, Virapandianpatnam, Thiruchendur 628 216, Thoothukudi District, Tamil Nadu, India
[c] Department of Chemistry, Division of Science and Humanities, Sree Sowdambika College of Engineering, Chettikurichi, Aruppukottai 626 134, Tamil Nadu, India
[d] Division of Science and Humanities, K.N.S.K. College of Engineering, Therekalputhoor, Nagercoil 629 001, Kanyakumari District, India

HIGHLIGHTS

- Substituted halopyrimidine derivatives are used in colorectal cancer chemotherapy.
- 5-Fluorouracil plays a crucial role in Food and Drug Administration systems.
- The metal complexes show homogeneous morphology with microcrystalline environment.
- Gel electrophoresis shows CT DNA undergoes oxidative cleavage with the complexes.
- *In vitro* antimicrobial and antioxidant assessments show high inhibiting potential.

GRAPHICAL ABSTRACT

Novel N_2O type mixed ligand complexes **(1–6)** have been synthesized from substituted fluoropyrimidine [5-Fluorouracil (5-FU: A)] with imidazole(him) and benzimidazole(bim) enzyme constituents(B) in the presence of M(II) ions [where M(II) = Ni(II), Cu(II) and Zn(II)]. Synthesized complexes **(1–6)** were characterized by chemical analysis and various spectral studies. *In vitro* antimicrobial activities of 5-Fluorouracil(A) and their mixed ligand complexes were screened against some bacterial and fungal strains by well diffusion technique. Electronic absorption and oxidative cleavage studies of the chelates with DNA under aerobic conditions show remarkable activities. Also, the absorption binding studies of CT DNA with the M(II)-5-FU(A)-him(B) complexes show decrease of 5–15% intensity with minor red shift along with significant hypochromicity and the free energy change values ($\Delta^{\ddagger}G$) indicate the M(II) complexes can interact with DNA in a spontaneous manner.

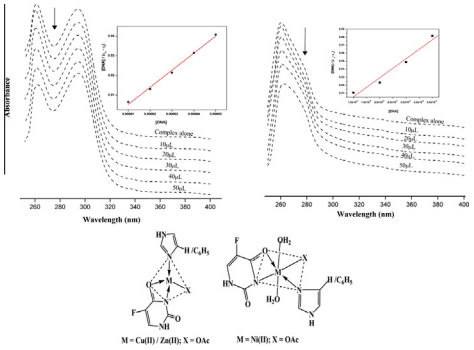

ARTICLE INFO

Article history:
Received 29 December 2013
Accepted 22 January 2014
Available online 18 February 2014

Keywords:
Fluoropyrimidine

ABSTRACT

Coordinating behavior of novel N_2O type mixed ligand complexes **(1–6)** have been synthesized from substituted fluoropyrimidine [5-Fluorouracil (5-FU; A)] with biopotent imidazole enzyme constituents (B) *viz.*, imidazole(him) and benzimidazole(bim) in the presence of Ni(II), Cu(II) and Zn(II) ions. Synthesized complexes were characterized by chemical analysis, spectral studies, magnetic moment and conductivity measurements. The results of chemical analysis and the observed low molar conductance values propose their stoichiometry to be 1:1:1 (M:A:B) with non-electrolytic nature. From the spectral data, it is inferred that the ligands A & B coordinate with M(II) ions in bi and monodentate approach

* Corresponding author. Tel.: +91 94435 00381; fax: +91 4639 245247.
E-mail addresses: Subramaniam.perumal@gmail.com, psubramaniam.ac@gmail.com (P. Subramaniam).

http://dx.doi.org/10.1016/j.saa.2014.01.089

Imidazole enzyme constituents
Mixed ligand complexes
Spectral studies
Pharmacological evaluation
DNA studies

through $C_{(4)}$=O, $N_{(3)}$ and imidazole ring $N_{(3)}$ atoms respectively. The thermogravimetric analysis shows the dehydration, decomposition and thermal stability of mixed ligand complexes. XRD and SEM patterns show sharp crystalline peaks with homogeneous morphology. *In vitro* antimicrobial activities of free ligands (A & B) and their metal complexes were screened against some pathogenic strains by well diffusion technique. Absorption and gel electrophoresis experiments on the interaction of mixed ligand complexes with DNA suggest that all the complexes can bind as well as cleave the DNA by intercalation between chromophores and DNA base pairs. In addition, *in vitro* antioxidant activities were tested by DPPH free radical scavenging model.

Introduction

The heterocyclic ring systems containing bioactive donor of N/O atoms present in pyrimidine moieties are the basic building blocks in modern drug designing architecture. These derivatives have occupied a unique and significant position in the field of medicinal, biological and therapeutical applications since they possess antibacterial, fungicidal, antitumor, antimitotic, antithyroid and surface anaesthesia activities [1,2]. Further, these derivatives are essential antimicrobial, antineoplastic, antiviral, antitumor, anti-HIV, antiinflammatory, antimalarial and cardiovascular agents in chemotherapeutical and agricultural areas [3–6]. They also bring into play an imperative role in hypnotic drugs for the nervous system, antagonists of the human A2A adenosine and calcium sensing receptors [7]. It is well known that pyrimidine derivatives of uracil, thymine and cytosine are the fundamental components in nucleic acids of DNA and RNA. In adjuvant chemotherapy, substituted pyrimidine derivatives alone or with leucovorin are functional to standard healing for high-risk Duke's C colon cancer (Stage II or Stage III). At very low concentration (<20 ppm), 5-Fluorouracil exhibits a cheerful inspiring effect on plant tumor growth which is produced by F1 hybrid of Nicotiana glauca Grah and Nicotiana langsdorffii Weinm [8]. Further, 5-Fluorouracil is a novel oral tumor-activated and tumor-elective fluoropyrimidine carbamate and an oral chemotherapeutic agent which is also used in the treatment of breast, esophageal and larynx, gastrointestinal and genitourinary tract cancers. The diazole ring moieties of imidazole derivatives are suggested as effective antifungal drugs (bifonazole, butoconazole, clotrimazole, miconazole, etc.,) and they possess some medicinal applications which include anticancer, β-lactamase inhibitors, antiaging agents, anticoagulants, antimalarial, antiinflammatory, antidiabetic and antitubercular activities [9,10]. Benzimidazole moiety acts as a fraction of the nucleotide fragment in vitamin B_{12} and in a range of biological and pharmacological actions [11].

Copper is an elementary micronutrient, necessary for all the living organisms and it is ubiquitous in catalytic co-factor for a range of metalloenzymes, electron transfer and oxygen transport proteins [12]. The copper containing proteins play a dynamic role in three major cellular processes namely amino acid metabolism, coagulation cascade and tyrosine metabolism with melanin biosynthesis. In addition to this, it concerned with many biological and physiological processes such as hemoglobin regulation, iron metabolism, mitochondrial respiration, biosynthesis of neurotransmitter, free radical detoxification, development of embryo and connective tissue, nerve coverings and bone [12]. Nickel is necessary to human and higher animal species like chickens, rats, pigs, cows, sheep and goats [13]. It also stabilizes DNA and RNA against thermal denaturation [13] and activates many enzymes. Zinc is the second richest trace element in human body which is intracellular in bone, muscle, skin, hair and liver [14]. It plays a chief role in all the biochemical pathways, perpetuation of genetic materials and in the function of retina, retinal pigment epithelium (RPE) and choroid.

The interactions of transition metal ions with DNA are significant, often changing the structure and function of genetic materials. Mixed ligand complexes have been introduced into DNA in order to gain the knowledge about the binding and/or cleaving mechanism, in particular to understand pre-requisites of specificity [15]. In addition, they have been used in the development of new target molecules for bio-reactivity of these metal complexes with DNA [16]. In absorption studies, the change in the intensities can be used to explain the nature and strength of the stacking interaction between chromospheres and DNA base pairs. In a sequel to our attempt [17–23], the novel N_2O type mixed ligand complex systems of Ni(II)/Cu(II)/Zn(II)-5-FU(A)-him/bim(B) were synthesised and characterized by means of analytical and spectral techniques. The *in vitro* antimicrobial and antioxidant activities of 5-Fluorouracil and their complexes have been studied. Electronic absorption and oxidative cleavage interaction of 5-Fluorouracil(A) and their metal complexes with DNA was also studied.

Experimental

Materials and reagents

All the ligands are extra pure Sigma Aldrich, Fluka (Puriss) products and they are used without further purification. Solvents for the physical measurements were of analytical grade and purified according to literature methods [24]. DNA was purchased from Genie (Bangalore, India), agarose (molecular biology grade) and ethidium bromides (EB) were obtained from Sigma Aldrich (USA). 2,2-diphenyl-1-picrylhydrazyl (DPPH) and ascorbic acid (AA) were purchased from Sigma Aldrich.

Instruments

Melting points (m.p.) of all the mixed ligand complexes were determined on Gallenkamp apparatus in open glass capillaries and are uncorrected. C, H and N analytical data were performed on Elementar Vario EL III CHNS analyzer. Metal content of the mixed ligand complexes were estimated gravimetrically by the standard procedure. Molar conductances of the mixed ligand complexes (1×10^{-3} mol) were measured using an Elico CM 180 conductivity bridge by using 0.01 M KCl solution as calibrant. Fast atomic bombardment mass spectra (FAB-MS) were recorded using a VGZAB-HS spectrometer in a 3-nitrobenzylalcohol matrix. Magnetic susceptibility measurements were carried out on a Gouy balance at room temperature using mercuric tetra(thiocyanato)cobaltate(II) as the calibrant. Diamagnetic corrections were applied in compliance with Pascal's constant [25]. Electronic absorption spectra were recorded with a Hitachi U-2000 double beam spectrophotometer in the 200–1100 nm range. Vibrational spectra were recorded using KBr pellets on a JASCO FT/IR-410 spectrometer, in the 4000–400 cm^{-1} range. ^1H NMR and ^{13}C NMR spectra of the diamagnetic Zn(II) complexes were carried out in DMSO-d_6 at room temperature using TMS as internal standard on

a Perkin Elmer R-32 spectrometer. X-band EPR spectra of Cu(II) complexes, at room temperature and liquid nitrogen conditions in DMSO medium, were recorded on a Varian ESR spectrometer using DPPH as internal standard. Thermal stabilities of the complexes were recorded in dynamic nitrogen atmosphere (flow rate 20 cm^3/min) with a heating rate of 10 K/min using a Perkin Elmer (TGS-2 model) thermal analyzer. Powder X-ray diffraction (XRD) patterns were recorded with a Bruker AXS D8 advance powder X-ray diffractometer (X-ray source: Cu, Wavelength 1.5406 Å) using Si(Li)PSD as the detector. Scanning Electron Micrography with Energy Dispersive Spectrometry associated (SEM/EDS) using JSM-5610 scanning electron microscope was used for morphological investigation.

In vitro antimicrobial activities

In vitro antimicrobial activities of 5-Fluorouracil(A) and their M(II)-5-FU(A)-him/bim(B) complexes in DMSO medium were tested against three Gram-positive pathogenic bacterial strains: *Bacillus subtilis*, *Staphylococcus saphyphiticus* and *Staphylococcus aureus*, two Gram-negative bacterial strains: *Escherichia coli* and *Pseudomonas aeruginosa* using Muller Hinton agar nutrient, and three fungal strains namely *Aspergillus niger*, *Enterobacter* species and *Candida albicans* using potato dextrose agar as the medium by well diffusion technique [26]. About 2–8 h, older microorganism species inoculums containing approximately 104–106 colony forming units (CFU) per cm^3 were used in these analyses. All the analyses were made in three replicate for each and the detailed procedure for measuring the zone of inhibition was followed as described earlier [18,19]. The results were recorded as zone of inhibition in mm and compared with the commercially available tetracycline and amphotricine, used as antibacterial and antifungal control respectively. Zone of inhibition is given as the average of three independent determinations.

In vitro antioxidant activity

In vitro antioxidant activities of 5-Fluorouracil(A) and their mixed ligand complexes have been tested under physiological conditions by DPPH (2,2-diphenyl-1-picrylhydrazyl) free radical scavenging assay method at 37 °C. DPPH free radical scavenging effect was carried out according to the Blois method [27]. The different concentrations of 5-Fluorouracil(A) (10, 20, 30, 40 and 50 μmol) and their metal complexes were prepared in DMSO medium. 1 cm^3 of each compound solution having different concentrations were taken in different test tubes and 4 cm^3 of a 0.1 mmol DPPH solution in DMSO was added to each test tube and the reaction mixture was shook vigorously for about 2–3 min. Each tube was then incubated in the dark room for 20–30 min at room temperature. A blank DPPH solution prepared without compound was used for the baseline correction. After incubation, the absorbance value of all compounds were measured at a (λ_{max}) of 517 nm, using an UV–vis. spectrophotometer. There was a decrease in the absorbance values (λ_{max}) which indicated that the mixed ligand complexes show moderate free radical scavenging activities. Ascorbic acid (AA) was used as the reference or positive control. Free radical scavenging effects in percentage was calculated using the formula,

$$\text{Scavenging effects } (\%) = \left[\frac{(A_{control} - A_{sample})}{A_{control}}\right] \times 100$$

where $A_{control}$ is the absorbance of the control without the ligand or the complex and A_{sample} is the absorbance of the ligand or the complex. All the analyses were made in three replicate for each and the results were compared with control.

Interaction between mixed ligand complexes with DNA

DNA experiments, with mixed ligand complexes in DMSO medium, were done in buffer (50 mmol Tris–HCl/NaCl, pH = 7.2) [28,29]. DNA concentration per nucleotide was determined by absorption spectroscopy using the molar absorption coefficient (ε = 6600 mol^{-1} cm^{-1}) at 260 nm. The purity of DNA was checked from its absorbance values at 260 and 280 nm and the ratio, A_{260}/A_{280}, was found to be indicating that CT DNA was sufficiently free from protein contamination [30]. Stock solution of CT DNA concentration per nucleotide [C(p)] in the buffer medium was measured from its absorption intensity at 260 nm after 1:100 dilution with known ε = 6600 mol^{-1} cm^{-1} value. Stock solutions were kept at 4 °C and used after not more than four days. Doubly distilled carbonate free water was used to prepare the buffer and other required solutions.

Absorption spectral titration experiments were done by keeping the concentration of mixed ligand complexes **(1–3)** as constant (30 mmol) while varying the CT DNA concentration ranged from 0 to 50 or more equivalents by maintaining the total volume of the solution as kept constant. After the addition of CT DNA, the resulting mixture was shaken up and allowed to equilibrate for 5–10 min at room temperature. The slow and successive additions of CT DNA to the complexes showed both hypochromicity and red-shifted charge transfer peak with maxima in the spectra. The titration processes were repeated until there was no change in the spectra indicating that binding saturation had been achieved. Absorption readings corresponding to the changes at maximum absorption with increasing concentration of CT DNA were recorded and the binding strength of mixed ligand complexes were evaluated quantitatively [31] as:

$$\frac{[DNA]}{(\varepsilon_a - \varepsilon_f)} = \frac{[DNA]}{(\varepsilon_b - \varepsilon_f)} + \frac{1}{K_b(\varepsilon_b - \varepsilon_f)}$$

where ε_f, ε_b and ε_a are the molar extinction coefficients of the free complex, completely bound form with CT DNA and with DNA respectively at a definite concentration. The observed absorption data was then fit into the above equation to obtain the intrinsic binding constant (K_b) by the plot of [DNA]/($\varepsilon_a - \varepsilon_f$) versus [DNA], where the slope and *y*-intercept of the above equation are $1/(\varepsilon_b - \varepsilon_f)$ and $1/K_b(\varepsilon_b - \varepsilon_f)$respectively. The intrinsic binding constant (K_b) was determined from the ratio of the slope to *y*-intercept.

Oxidative DNA cleavage studies

DNA cleavage activities of 5-Fluorouracil(A) and their mixed ligand complexes were monitored by agarose gel electrophoresis on CT DNA. Gel electrophoresis experiments were performed under aerobic condition with an oxidant (H_2O_2) by incubation at 35 °C for 2 h as follows: CT DNA 30 μmol, 50 μmol of each complex, 50 μmol of oxidant in 50 mmol Tris–HCl/NaCl buffer (pH = 7.2) containing 50 mmol NaCl solutions. After incubation, 1 μcm^3 of loading buffer (bromophenol blue in water) was added to each tube and the samples were loaded on 1% agarose gel. Samples were electrophoresed at a constant voltage (50 V) for 2 h in Tris–acetic acid–EDTA buffer (pH 8.3). After electrophoresis, the gel was stained for 30 min by immersing it in 1 μg/cm^3 ethidium bromide (EB) solution. DNA cleavage were visualized by viewing the gel under Ultraviolet (UV) light and photographed.

*General procedure for synthesis of mixed ligand complexes **(1–6)***

All the six mixed ligand complexes were synthesised by the following general procedure: 5-Fluorouracil (0.013 g, 10 mmol) was dissolved in aqueous (10 cm^3) solution containing a few drops

of concentrated ammonia and get a clear solution on stirring. An appropriate metal salt solution (10 cm^3) of 10 mmol, 0.025 g $Ni(CH_3COO)_2{\cdot}4H_2O$ or 0.020 g $Cu(CH_3COO)_2{\cdot}H_2O$ or 0.022 g Zn $(CH_3COO)_2{\cdot}2H_2O$), was added dropwise to the above solution and stirred at room temperature (Scheme 1). To this, aqueous solution (10 cm^3) of imidazole (0.007 g, 10 mmol) or benzimidazole (0.012 g, 10 mmol) was added and the reaction mixture was refluxed for 6–8 h on a water bath. The pH (6.8) of the reaction mixture was adjusted by adding few drops of aqueous Na_2CO_3 solution. The resulting solutions were reduced to 1/3 of its original volume and kept aside. On standing, the mixed ligand complexes were obtained and collected by vacuum filtration, washed several times with cold water, ethanol and anhydrous ether. The mixed ligand complexes were obtained as powder and dried in air and stored in vacuo over anhydrous $CaCl_2$ at room temperature. The yield of the isolated complexes were found to be 60–75%.

*Complex **(1)**. [5-Fluoro-8,8-dihydroxy-8-(3H-1λ^4,3-imidazol-3-yl)-2-oxo-7λ^3-oxa-1,3-diaza-8-nickel(II)abicyclo[4.2.0]octa-4,6-dien-8-yl acetate]*

Yield: 68%; m.p.: 247 °C; Color: Lustrous dark green; Mol. for.: $[C_9H_{13}FN_4O_6Ni]$; Mol. wt.: 350.92; Selected FT-IR data in cm^{-1} (KBr disk): $\bar{\nu} = 3600—3500, 1515, 1409$ (br, ν(NH) vib. of N_1H & N_3H group in 5-FU), 3450–3300, 846, 716 (br, OH_2 molecule), 3375, 1472 (br, NH, imidazole ring), 1698 and 1666 (d, C═O str., pyrimidine ring), 1568 (s, C═N, imidazole ring), 1575 and 1358 (m, —COO, acetate group), 1472 (m, C_5—F vib. of 5-FU), 522 (w, Ni—N), 461 (w, Ni—O); FAB-MS: m/z = 352.01 [M + 1]; UV–vis., (10^{-3} mol in DMSO): λ_{max} = 32,258, 25,840, 17,153 and 10,362 cm^{-1}; μ_{eff} = 3.09 BM; Λ_M (10^{-3} mol in DMSO) = 18.19 S cm^2 mol^{-1}.

*Complex **(2)**. [5-Fluoro-8-(3H-1λ^4,3-imidazol-3-yl)-2-oxo-7λ^3-oxa-1,3-diaza-8-cupra(II)abicyclo[4.2.0]octa-4,6-dien-8-yl acetate]*

Yield: 70%; m.p.: 266 °C; Color: Pale brown; Mol. for.: $[C_9H_9FN_4O_4Cu]$; Mol. wt.: 319.74; Selected FT-IR data in cm^{-1} (KBr disk): = 3600–3500, 1514, 1406 (br, ν(NH) vib. of N_1H & N_3H group in 5-FU), 3372, 1473 (br, NH, imidazole ring), 1695 and 1653 (d, C═O str., pyrimidine ring), 1572 (s, C═N, imidazole ring), 1585 and 1362 (m, —COO, acetate group), 1473 (m, C_5—F vib. of 5-FU), 538 (w, Cu—N), 470 (w, Cu—O); FAB-MS: m/z = 320.98 [M + 1]; UV–vis., (10^{-3} mol in DMSO): λ_{max} = 26,455 and 13,441 cm^{-1}; μ_{eff} = 1.96 BM; Λ_M (10^{-3} mol in DMSO) = 19.62 S cm^2 mol^{-1}.

*Complex **(3)**. [5-Fluoro-8-(3H-1λ^4,3-imidazol-3-yl)-2-oxo-7λ^3-oxa-1,3-diaza-8-zinc(II)abicyclo[4.2.0]octa-4,6-dien-8-yl acetate]*

Yield: 68%; m.p.: 278 °C; Color: Lustrous colorless; Mol. for.: $[C_9H_9FN_4O_4Zn]$; Mol. wt.: 321.60; Selected FT-IR data in cm^{-1} (KBr disk): $\bar{\nu} = 3600—3500, 1516, 1411$ (br, ν(NH) vib. of N_1H & N_3H group in 5-FU), 3374, 1470 (br, NH, imidazole ring), 1699 and 1671 (d, C═O str., pyrimidine ring), 1566 (s, C═N, imidazole ring), 1560 and 1341 (m, —COO, acetate group), 1470 (m, C_5—F vib. of 5-FU), 521 (w, Zn—N), 455 (w, Zn—O); FAB-MS: m/z = 322.91 [M + 1]; UV–vis., (10^{-3} mol in DMSO): λ_{max} = 26,738 cm^{-1}; μ_{eff} = Diamagnetic; Λ_M (10^{-3} mol in DMSO) = 20.15 S cm^2 mol^{-1}.

*Complex **(4)**. [5-Fluoro-8,8-dihydroxy-8-(3H-1λ^4,3-benzodiazol-3-yl)-2-oxo-7λ^3-oxa-1,3-diaza-8-nickel(II)abicyclo[4.2.0]octa-4,6-dien-8-yl acetate]*

Yield: 68%; m.p.: 243 °C; Color: Lustrous dark green; Mol. for.: $[C_{13}H_{15}FN_4O_6Ni]$; Mol. wt.: 400.97; Selected FT-IR data in cm^{-1} (KBr disk): $\bar{\nu} = 3600—3500, 1512, 1415$ (br, ν(NH) vib. of N_1H & N_3H group in 5-FU), 3450–3300, 835, 729 (br, OH_2 molecule), 3353, 1456 (br, NH, imidazole ring), 1701 and 1659 (d, C═O str., pyrimidine ring), 1537 (s, C═N, imidazole ring), 1570 and 1347 (m, —COO, acetate group), 1468 (m, C_5—F vib. of 5-FU, 518 (w, Ni—N), 457 (w, Ni—O) cm^{-1}; FAB-MS: m/z = 402.03 [M + 1]; UV–vis., (10^{-3} mol in DMSO): λ_{max} = 33,898, 26,455, 16,920 and 10,225 cm^{-1}; μ_{eff} = 3.15 BM; Λ_M (10^{-3} mol in DMSO) = 19.53 S cm^2 mol^{-1}.

*Complex **(5)**. [5-Fluoro-8-(3H-1λ^4,3-benzodiazol-3-yl)-2-oxo-7λ^3-oxa-1,3-diaza-8-cupra(II)abicyclo[4.2.0]octa-4,6-dien-8-yl acetate]*

Yield: 74%; m.p.: 250 °C; Color: Pale brown; Mol. for.: $[C_{13}H_{11}FN_4O_4Cu]$; Mol. wt.: 369.80; Selected FT-IR data in cm^{-1} (KBr disk): $\bar{\nu} = 3600—3500, 1517, 1411$ (br, ν(NH) vib. of N_1H & N_3H group in 5-FU), 3351, 1454 (br, NH, imidazole ring), 1705 and 1662 (d, C═O str., pyrimidine ring), 1541 (s, C═N, imidazole ring), 1566 and 1348 (m, —COO, acetate group), 1471 (m, C_5—F vib. of 5-FU), 539 (w, Cu—N), 466 (w, Cu—O) cm^{-1}; FAB-MS: m/z = 371.01 [M + 1]; UV–vis., (10^{-3} mol in DMSO): λ_{max} = 25,707 and 13,680 cm^{-1}; μ_{eff} = 1.94 BM; Λ_M (10^{-3} mol in DMSO) = 20.39 S cm^2 mol^{-1}.

*Complex **(6)**. [5-Fluoro-8-(3H-1λ^4,3-benzodiazol-3-yl)-2-oxo-7λ^3-oxa-1,3-diaza-8-zinc(II)abicyclo[4.2.0]octa-4,6-dien-8-yl acetate]*

Yield: 72%; m.p.: 263 °C; Color: White; Mol. for.: $[C_{13}H_{11}FN_4O_4Zn]$; Mol. wt.: 371.66; Selected FT-IR data in cm^{-1} (KBr disk): $\bar{\nu} = 3600—3500, 1514, 1408$ (br, ν(NH) vib. of N_1H & N_3H group in 5-FU), 3354, 1457 (br, NH, imidazole ring), 1703 and 1676 (d, C═O str., pyrimidine ring), 1535 (s, C═N, imidazole ring), 1545 and 1321 (m, —COO, acetate group), 1469 (m, C_5—F vib. of 5-FU), 512 (w, Zn—N), 451 (w, Zn—O) cm^{-1}; FAB-MS: m/z = 372.04 [M + 1]; UV–vis., (10^{-3} mol in DMSO): λ_{max} = 27,624 cm^{-1}; μ_{eff} = Diamagnetic; Λ_M (10^{-3} mol in DMSO) = 21.85 S cm^2 mol^{-1}.

Results and discussion

*Physico-chemical properties of the metal complexes **(1–6)***

The synthesised mixed ligand complexes are highly air-stable and non-hygroscopic in nature. They are insoluble in water and in common organic solvents like benzene, acetone, petroleum ether etc., but soluble in DMSO, DMF and Dioxan. The obtained chemical analysis (C, H, N) result with its molecular formula and other spectral data values are summarized in the experimental part. From the analytical data, the stoichiometry of M(II): 5-Fluoro-uracil: imidazole/benzimidazole is to be 1:1:1 in MAB type

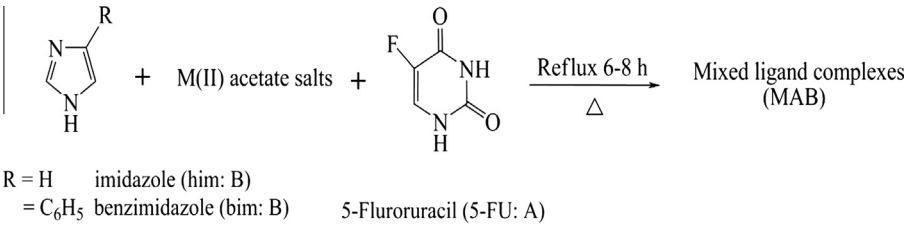

Scheme 1. Formation of mixed ligand complexes (MAB).

complexes and this analytical values are in good concord with the calculated values (Table 1). The observed low molar conductance values of the metal complexes (1×10^{-3} mol, DMSO solution) at room temperature are reliable with the non-electrolytic nature due to the absence of counter ions in the proposed structures [32]. Fast atomic bombardment mass spectrum (FAB-MS) of the synthesized mixed ligand complexes show the molecular ion (m/z) peaks which confirms the stoichiometry [M(II)-5-FU(A)-him/bim(B)$(OAc)(OH_2)_{x=0/2}$] of the metal chelates. This type of stoichiometry is further confirmed by the observed analytical and their spectral data of the metal chelates.

Infrared spectra with mode of binding

The characteristic IR spectral data (KBr pellet, cm^{-1}) of Ni(II)/Cu(II)/Zn(II)-5-FU(A)-him/bim(B) complexes were represented in the experimental part. In order to study the mode of coordination between free ligands (A & B) with the M(II) ions in mixed ligand complexes, the IR spectrum of 5-FU(A) and him/bim(B) ligands were compared to the spectra of their mixed ligand complexes and are listed in Table 2. From the data, it is found that 5-FU(A) acts as bidentate which form metal chelates through the deprotonated N_3 and C_4═O of carbonyl oxygen atoms. Similarly, him/bim(B) ligands bind the M(II) ions in unidentate manner via imidazole ring —N_3 atom. In addition, two new peaks were appeared in the far infrared region at 470–451 cm^{-1} and 539–512 cm^{-1} for ν(M—O) and ν(M—N) modes respectively [33,34]. This ν(M—O) and ν(M—N) peak values follow Irving-William order of stability as: Cu > Ni > Zn and also in comparable with the crystal field stabilization energies [35]. The Ni(II)-5-FU(A)-him/bim(B) complexes show a broad peak in the region 3450–3300 cm^{-1} and new peaks appeared in 846–835 cm^{-1} and 739–716 cm^{-1} are attributed to the stretching, rocking and wagging mode of ν(OH) vibration of the coordinated water (OH_2) molecule in the complexes [33,34]. The absence of coordinated water molecules in the heated synthesised complexes **(1 & 4)** at 85–140 °C is further confirmed from the absence of any broad band in the IR spectra around at ca. 3450–3300 cm^{-1}.

Also, all these complexes show an additional characteristic bands in the region 1585–1545 cm^{-1} and 1362–1321 cm^{-1} are ascribed to ν(C—O) of asymmetric and symmetric vibration of the acetate (COO^-) group respectively [33], indicating the participation of the carboxylate oxygen in the mixed ligand complex formation. The magnitude of $\Delta\nu$ values fall in the range 224–217 cm^{-1} suggesting the unidentate coordination of carboxylate acetate (OAc) group in the complexation. Based on the conductivity measurements, magnetic moment, spectral studies (IR spectra, ^1H & ^{13}C NMR spectra) and thermal analyses of mixed ligand complexes, we confirm that Ni(II) complexes **(1 & 6)** are of distorted octahedral environment with a stoichiometry of [Ni(II)-5-FU(A)-him/bim(B)$(OH_2)_2(OAc)$] and Cu(II)/Zn(II) complexes are distorted tetrahedral geometry with [M(II)-5-FU(A)-him/bim(B)(OAc)] stoichiometry.

Electronic absorption spectra coupled with magnetic moment values

The electronic absorption spectra of complexes were recorded in (1×10^{-3} mol) DMSO medium at room temperature (Fig. 1) and the electronic absorption spectral data of the mixed ligand complexes are presented in Table 3. Also, various spectral parameters (B, B′, β, β (%) and LFSE) for the Ni(II) complexes are calculated by applying band energies on Tanabe–Sugano diagrams.

Ni(II)-5-FU(A)-him/bim(B) complexes display four spin allowed bands at 33,898–32,258, 26,455–25,840, 17,153–16,920 and 10,362–10,225 cm^{-1}, which may be due to LMCT ($n \rightarrow \pi^*$), $^3A_{2g}(F) \rightarrow {}^3T_{1g}(P)$, $^3A_{2g}(F) \rightarrow {}^3T_{1g}(F)$ and $^3A_{2g}(F) \rightarrow {}^3T_{2g}(F)$ transitions respectively, with an distorted octahedral geometry with $^3A_{2g}$ as ground state [36,37]. The ratio of ν_2/ν_1 values lie in between 1.66 and 1.65, as expected for octahedral geometry, and the magnetic moment values, 3.09 and 3.15 BM for the complexes indicating two unpaired electrons with the high spin six-coordinated octahedral environment around the Ni(II) ion [36].

The copper complexes **(2 & 5)** exhibit one LMCT band, at 26,455 cm^{-1} for Cu(II)-5-FU(A)-him(B) and at 25,707 cm^{-1} for Cu(II)-5-FU(A)-bim(B) complex and an unsymmetrical broad absorption band which is centered at 13,441 and 13,680 cm^{-1} respectively that can be assigned to d–d electronic transition [36]. Such type of low energy absorption band with less intensity is commonly found in distorted tetrahedral environment which is caused by Jahn–Teller distortion. The observed magnetic moment values, 1.96 and 1.94 BM are also well agreed within the predictable region of 1.92–2.00 BM, found for distorted tetrahedral environment [36,37]. However, the complexes of Zn(II)-5-FU(A)-him/bim(B) show one broad band middled at 26,738 and 27,624 cm^{-1} respectively in the UV region due to L → M charge transfer transition in tetrahedral environment. Further, due to diamagnetic nature of Zn(II) ion, Zn(II) complexes do not show any d–d transitions in the visible region [36,37].

From Tanabe–Sugano diagrams, the stabilization parameters like ligand field splitting energy (Dq), Racah interelectronic repulsion parameter (B), the nephelauxetic ratio (β), percentage of covalency (% β) and LFSE values for Ni(II)-5-FU(A)-him/bim(B) complexes **(1 & 4)** were calculated and the values are 1036 and 1022 cm^{-1}, 793.62 and 846.71, 0.77 and 0.82, 22.95 and 17.79, and 145.83 and 146.88 kJ mol^{-1} respectively for complexes Ni(II)-5-FU(A)-him/bim(B) complexes. The observed ligand field parameters and magnetic moment values also support the covalent character of distorted octahedral geometry around the Ni(II) ion with D_{4h} symmetry [38,39]. Also, due to the mixing of ground state ($^3A_{2g}$) with the excited state ($^3T_{2g}$) in octahedral Ni(II) complexes give the Lunde's factor, i.e., $g = 2 - \frac{8\lambda'}{10Dq}$, (where λ' = spin-orbit coupling constant, -368 cm^{-1}). In general, the hexaaquo Ni(II) complexes show the g value of 2.25 [38], while Ni(II)-5-FU(A)-him/bim(B) complexes **(1 & 4)** show the g values of 2.246 and 2.252 respectively which supports the octahedral environment around the Ni(II) ions.

Table 1
Elemental analysis, molar conductivity and melting point of mixed ligand complexes **(1–6)**.

Compound	Color	Empirical Formula	Yield (%)	Elemental analysis, found (calculated) %				Λ_m (S cm^2 mol^{-1})	m.p. (°C)
				M	C	H	N		
(**1**)	Lustrous dark green	$NiC_9H_{13}FN_4O_6$	68	16.59 (16.73)	30.68 (30.80)	3.54 (3.73)	16.14(15.97)	18.19	247
(**2**)	Pale brown	$CuC_9H_9FN_4O_4$	70	19.52 (19.87)	33.45 (33.81)	2.63 (2.84)	17.28 (17.52)	19.62	266
(**3**)	Lustrous colorless	$ZnC_9H_9FN_4O_4$	68	20.10 (20.34)	33.38 (33.61)	2.66 (2.82)	17.15 (17.42)	20.15	278
(**4**)	Lustrous dark green	$NiC_{13}H_{15}FN_4O_6$	68	14.28 (14.64)	38.56 (38.94)	3.58 (3.77)	13.76 (13.97)	19.53	243
(**5**)	Pale brown	$CuC_{13}H_{11}FN_4O_4$	74	16.95 (17.18)	41.96 (42.22)	2.86 (3.00)	14.89 (15.15)	20.39	250
(**6**)	White	$ZnC_{13}H_{11}FN_4O_4$	72	17.41 (17.60)	41.89 (42.01)	2.73 (2.98)	14.87 (15.07)	21.85	263

Table 2
IR spectral data (in cm^{-1}) of 5-Fluorouracil(A), imidazole(B), benzimidazole(B) and their mixed ligand complexes **(1–6)**.

Complex	ν(M—O)	ν(M—N)	ν(OH_2)	ν(C=O) of C_2 and C_4 pyrimidine ring	δ(N—H) of N_1 and N_3 pyrimidine ring	ν(C_5—F) pyrimidine ring	ν(N_1—H) imidazole ring	ν(C=N) imidazole ring	ν(COO^-)$_{as}$	ν(COO^-)$_s$
5-Fluorouracil(5-FU: A)	–	–	–	1704, 1685	1513, 1430	1470	–	–	–	–
Imidazole(him: B)	–	–	–	–	–	–	3380, 1475	1585	–	–
Benzimidazole(bim: B)	–	–	–	–	–	–	3355, 1460	1552	–	–
Ni(II)-5-FU(A)-him(B)	461	522	3450–3300, 846, 716	1698, 1666	1515,1409	1472	3375, 1472	1568	1575	1358
Cu(II)-5-FU(A)-him(B)	470	538	–	1695, 1653	1514, 1406	1473	3372, 1473	1572	1585	1362
Zn(II)-5-FU(A)-him(B)	455	521	–	1699, 1671	1516,1411	1470	3374, 1470	1566	1560	1341
Ni(II)-5-FU(A)-bim(B)	457	518	3450–3300, 835, 729	1701, 1659	1512,1415	1468	3353. 1456	1537	1570	1347
Cu(II)-5-FU(A)-bim(B)	466	539	–	1705, 1662	1517,1411	1471	3351,1454	1541	1566	1348
Zn(II)-5-FU(A)-bim(B)	451	512	–	1703, 1676	1514,1408	1469	3354,1457	1535	1545	1321

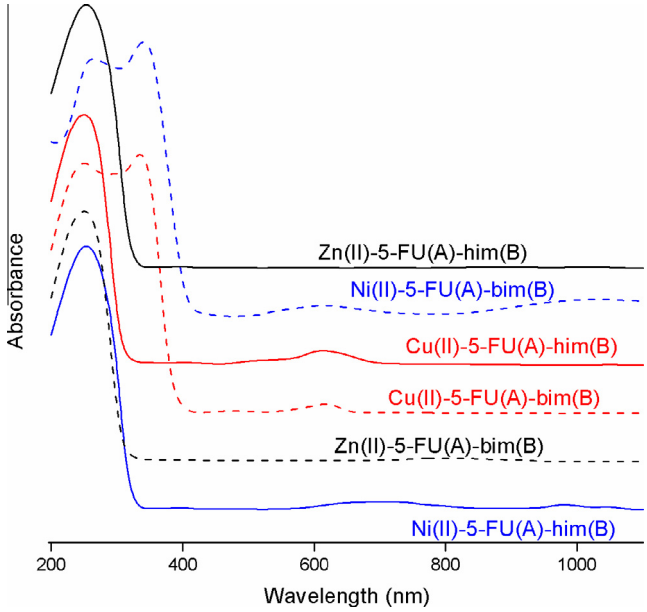

Fig. 1. Electronic absorption spectra of M(II)-5-FU(A)-him/bim(B) complexes (1–6) in DMSO medium at room temperature (10^{-3} mol).

*^{1}H and ^{13}C NMR spectra of Zn(II) complexes **(3 & 6)***

Both ^{1}H and ^{13}C NMR spectra of diamagnetic Zn(II)-5-FU(A)-him/bim(B) complexes **(3 & 6)** were recorded in DMSO-d_6 using tetramethylsilane (TMS) as internal standard at room temperature. The representative structure of the Zn(II)-5-FU(A)-him/bim(B) complexes **(3 & 6)** are compared with the free ligands, 5-FU(A) and him/bim(B) which are shown in Fig. 2. All the protons are established to be in their predictable regions [39]. From the NMR spectra it is proved that the 5-FU(A) and him/bim(B) ligands act as bi and monodentate coordination around the Zn(II) ion via, deprotonated —N_3, carbonyl oxygen (—C_4=O) and imidazole ring —N_3, atoms respectively. In addition, there is a peak found at δ = 1.81 and 1.85 ppm in the metal chelates indicate that the acetate (OAc) molecule is coordinated with the Zn(II) ion [39]. Thus monodentate acetate ion can act as one of the ligating agent and binds in the inner coordination sphere of the mixed ligand complexes. This is further confirmed from the observed molar conductivity values *i.e.,* non-electrolytic nature of the complexes. Thus, the NMR study of Zn(II) complexes confirm the conclusions drawn from the IR spectra on the mode of binding of the ligands.

*EPR spectra of Cu(II) complexes (**2 & 5**)*

EPR spectra of polycrystalline Cu(II)-5-FU(A)-him/bim(B) complexes **(2 & 5)** were recorded on X-band at ambient and low (300–77 K) temperatures in DMSO medium and the EPR spectrum of Cu(II)-5-FU(A)-him(B) complex is shown in Fig. S1 (Supplementary data file). At 300 K, the EPR spectra of the complexes exhibit well-resolved hyperfine structures due to magnetic coupling between the unpaired electron with effective ^{63,65}Cu nuclei (I = 3/2). In the case of frozen solution (77 K), the spectra show anisotropic pattern for the powder samples in the parallel and perpendicular regions, *i.e.,* four well-resolved peaks and this may be assignable to monomeric nature of the complexes [40]. This is further supported from the observed magnetic moment values of the Cu(II) complexes in solid state. Axial symmetric with g-tensor values of Hamiltonian parameters follow the order as: $g_{\|}$ (2.15) > $g_{\perp}$ (2.04) > g_e (2.0023) for complex **(2)** and $g_{\|}$ (2.11) > $g_{\perp}$ (2.03) > g_e (2.0023) for complex **(5)** respectively. It clearly indicates that the unpaired electron is localized in $d_{x^2-y^2}$ orbital [40] with $3d^9$ configuration. The observed g-tensor values are less than 2.3, indicating considerable covalent environment in the Cu—L bond [40] which is in conformity with the presence of mixed Cu—N and Cu—O bonds in chelates. Further, the deviation of calculated g-tensor values 2.08 and 2.05 from the free electron value (g_e = 2.0023) supports the covalent property. The absence of any half field signal at 1600 G corresponding to ΔM_s = ±2 transitions, ruling out any magnetic exchange i.e., Cu—Cu interactions in the complexes.

Bonding parameter values (α^2 = 0.59 & 0.61 and β^2 = 0.89 & 0.87) clearly indicate that the σ – bonding is more covalent than in-plane π – bonding [41,42]. Also the observed $A_{\|}$ values (138 and 132 × 10^{-4} cm) are comparable to the reported distorted tetrahedral Cu(II) complexes [42]. The geometry of the complexes **(2 & 5)** are further inveterate by the empirical factor (f) i.e., $f = \frac{g_{\|}}{A_{\|}}$, an index of tetragonal distortion. The reported (f) value for N_2O donor groups around the copper ion for square planar com-

Table 3
Absorption spectral data (in DMSO) and the magnetic moment values of mixed ligand complexes **(1–6)**.

Complex	λ_{max} (cm^{-1})	Band assignments	Geometry	μ_{eff} (BM)	Ligand field parameter					
					Dq (cm^{-1})	B (cm^{-1})	β	β (%)	LFSE (kJ mol^{-1})	ν_2/ν_1
Ni(II)-5-FU(A)-him(B)	10,362 17,153 25,840 32,258	$^3A_{2g}(F) \rightarrow {}^3T_{2g}(F)$ $^3A_{2g}(F) \rightarrow {}^3T_{1g}(F)$ $^3A_{2g}(F) \rightarrow {}^3T_{1g}(P)$ LMCT ($n \rightarrow \pi^*$)	Distorted octahedral	3.09	1036	793.62 (B′ for free Ni(II) ion = 1030)	0.77	22.95	145.83	1.66
Cu(II)-5-FU(A)-him(B)	13,441 26,455	d–d Envelope LMCT ($n \rightarrow \pi^*$)	Distorted tetrahedral	1.96	–	–	–	–	–	–
Zn(II)-5-FU(A)-him(B)	26,738 (b)	LMCT (M ← N)	Distorted tetrahedral	Dia.	–	–	–	–	–	–
Ni(II)-5-FU(A)-bim(B)	10,225 16,920 26,455 33,898	$^3A_{2g}(F) \rightarrow {}^3T_{2g}(F)$ $^3A_{2g}(F) \rightarrow {}^3T_{1g}(F)$ $^3A_{2g}(F) \rightarrow {}^3T_{1g}(P)$ LMCT ($n \rightarrow \pi^*$)	Distorted octahedral	3.15	1022	846.71	0.82	17.79	146.88	1.65
Cu(II)-5-FU(A)-bim(B)	13,680 25,707	d–d Envelope LMCT ($n \rightarrow \pi^*$)	Distorted tetrahedral	1.94	–	–	–	–	–	–
Zn(II)-5-FU(A)-bim(B)	27,624 (b)	LMCT (M ← N)	Distorted tetrahedral	Dia.	–	–	–	–	–	–

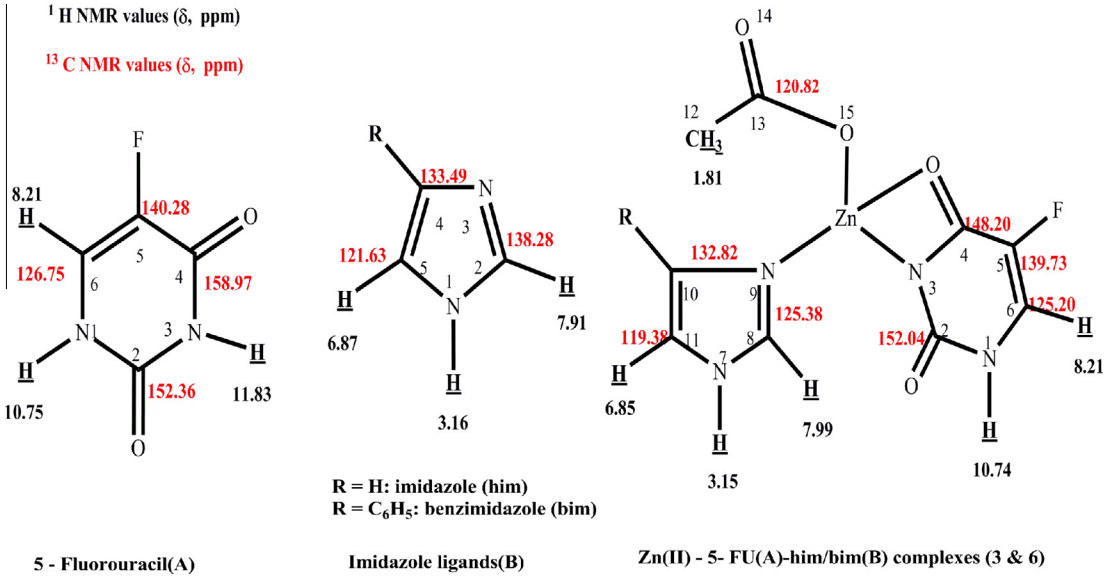

Fig. 2. ^{1}H NMR and ^{13}C NMR of the free ligands (A & B) and their Zn(II)-5-FU(A)-him/bim(B) complexes (**3 & 6**) in DMSO-d_6 medium at room temperature.

plexes are in the order of 100–125 × 10^{-4} cm where as in Cu(II) complexes (**2 & 5**) the observed (f) value is in the range, 130–150 × 10^{-4} cm and the calculated empirical factor value (f = 156 and 159 × 10^{-4} cm) confirm distorted tetrahedral arrangement. This is in agreement with the other reported values for distorted tetrahedral environment around the copper(II) complexes [41,42]. This is further supported from the calculated G-tensor value [43], which is a measure of the exchange interaction between metal centers in polycrystalline states, is calculated by using the expression $\left[G = \frac{(g_{\parallel} - g_e)}{(g_{\perp} - g_e)}\right]$. Since the observed G values (3.92 and 3.89) are <4, the exchange interaction is considerable in the present case and it may be due to the aligned parallel or slightly misaligned environment of local tetragonal axes [43].

Thermogravimetric analyses

Thermogravimetric analyses were performed for Ni(II)-5-FU(A)-him(B) and Zn(II)-5-FU(A)-bim(B) complexes **(1 & 6)** in the temperature range of ambient to 1100 °C under stable air condition. Thermal decomposition of the metal complexes **(1 & 6)** occur in four and three steps respectively. In Ni(II)-5-FU(A)-him(B) complex **(1)**, the first loss in weight occurs in the range of 80–150 °C, indicating the presence of coordinated water molecules (H_2O). These results explain accordingly the analytical suggestions [44,45], *i.e.,* (i) Lattice water, free ions and organic fragments that are not directly coordinated to the metal ions are found to leave the complex at earlier stages compared with coordinated fragments, (ii) The heating range (ambient to 1100 °C temperature) produces incomplete decomposition of M(II) complexes and (iii) the final products are dependent on the type of M(II) ion and on (M → L) affinity which reflects the stability of complexes [44].

In the decomposition of Ni(II) complex **(1)**, the first step corresponds to the removal of two coordinated water molecules followed by the removal of one acetate moiety in the second step. In the third and fourth steps, the subsequent elimination of imidazoles (B) and 5-Fluorouracil(A) ligand moieties take place and

finally it leaves air stable metal oxide (Ni—O) as residue [44] at very high temperatures, above 720 °C. The results are well agreed with the composition of metal chelate and the final product is confirmed by IR studies. The thermogravimetric degradation of Ni(II) complex **(1)** is represented in Scheme 2.

The Zn(II)-5-FU(A)-bim(B) complex **(6)** does not show any loss in weight up to 180 °C, reveals that crystal water molecules or coordinated water molecules are absent in the complex [45]. Also, at 180 °C, the complex is further analysed by IR spectral studies and their IR spectra exhibits absence of any broad band around at *ca.* 3450–3300 cm^{-1} which confirms the absence of water molecule in this complex. The TGA/DTA diagram of Zn(II)-5-FU(A)-bim(B) complex **(6)** is shown in Fig. S2 (Supplementary data file). The decomposition of Zn(II) complex **(6)** occurs in three steps. The first step corresponds to the removal of coordinated acetate moiety followed by the subsequent elimination of ligands, benzimidazole (B) and 5-Fluorouracil(A) at 294–343.71 and 382–417.53 °C respectively. Finally, it leaves the air stable metal oxide (Zn—O) as residue at very high temperatures from 700 °C onwards. The results are in accord with the composition of metal chelates. Further, the kinetic order of decomposition was calculated by the modified Horowitz and Metzger equation [46], $\left[C_s = \frac{(W_s - W_f)}{(W_o - W_f)}\right]$ and the observed C_s values (0.64–0.60) of the mixed ligand complexes (**1 & 6**) indicate that the decomposition follows first order kinetics.

Based on the conductivity measurements, magnetic moment, spectral studies (IR spectra, ^1H and ^{13}C NMR spectra) and thermal analyses of mixed ligand complexes **(1–6)**, it is confirmed that Ni(II) complexes (**1 & 4**) have distorted octahedral environment with stoichiometry [Ni(II)-5-FU(A)-him/bim(B)$(OH_2)_2$ (OAc)] while Cu(II)/Zn(II) complexes have distorted tetrahedral geometry with [M(II)-5-FU(A)-him/bim(B)(OAc)] stoichiometry (Fig. 3).

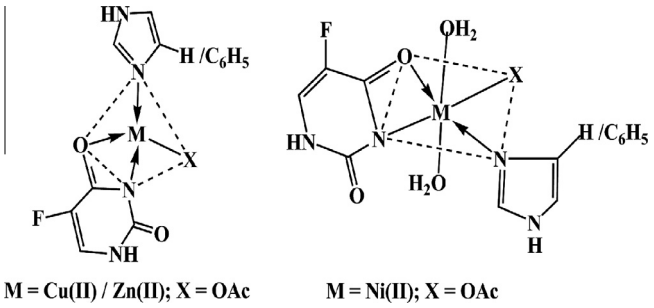

Fig. 3. Proposed structure of M(II)-5-FU(A)-him/bim(B) complexes **(1–6)**.

Powder X-ray diffraction and SEM analysis

Powder X-ray diffraction studies and SEM analysis are useful to determine the structure, particle size and morphology of the synthesized mixed ligand complexes. The X-ray diffractogram of the synthesised mixed ligand complexes of Ni(II)/Cu(II)/Zn(II)-5-FU(A)-him(B) complexes **(1–6)** are shown in Fig. 4.

The observed d-space values for the mixed ligand complexes are compared with the standard d-space values of the free metal(II) ions, free ligands (A & B), M(II)-5-substituted uracil derivatives, Ni(II)-$(him)_2$ $(NO_3)_2$ and Cu(II)-$(him)_2$ Cl_2 complexes from JCPDS data files. The experimental d-space values of the mixed ligand complexes match with the JCPDS data d-space values which are shown in Table S1 (Supplementary data file) which confirm the presence of 5-FU(A), imidazoles(B) moiety and acetate/water molecules in the mixed ligand complexes [47].

In the diffractogram, the strong peaks corresponding to $2(\theta)$ appeared at 18.6, 25.6 and 34.8, for Ni(II) complex **(1)**, at13.5, 22.5 & 29.8 for Cu(II) complex **(2)** and at 11.8, 19.6 & 28.7 for Zn(II) complex **(3)**, confirm the mixed ligand complex formation. Also there are a large number of feeble peaks observed in the mixed ligand complexes indicate uniform phase with no impurity. The XRD pattern shows microcrystalline nature of the complexes and this behavior is due to the incorporation of water and acetate molecules into the coordination sphere. The average crystalline size of the synthesised mixed ligand complexes are found to be 57.9 nm, 66.6 nm and 61.8 nm for Ni(II), Cu(II) and Zn(II) respectively as calculated from the main X-ray diffraction peaks using the Scherre's equation [47],

$$D = 0.9\lambda/\beta\cos\theta$$

where λ is the wavelength of X-ray radiation (λ = 0.154 nm), β is the full width half maximum of the characteristic peak (in radians) corrected for instrumental broadening, θ is Bragg diffraction angle for hkl plane and D is the crystalline size (nm). This crystalline value suggests that the synthesized mixed ligand complexes are in microcrystalline state which confirms the proposed composition.

Morphology and particle size of the MAB type mixed ligand complexes of Ni(II) and Cu(II)-5-FU(A)-bim(B) complexes **(4 & 5)** were illustrated from the scanning electron microscopic pictograph (Fig. 5). From the SEM pictographs, it is inferred that the mixed ligand complexes have uniform matrix with smooth interface having perfect regular shape of homogeneous phase material. A mixture of wrecked brick and crumb like shapes is observed in the Ni(II) complex **(4)** with the particle size 35 μm. Particle size of Cu(II) complex **(5)** is obtained as 20 μm with huge structure of regular micro-crystalline shape of germ like phase. This leads to

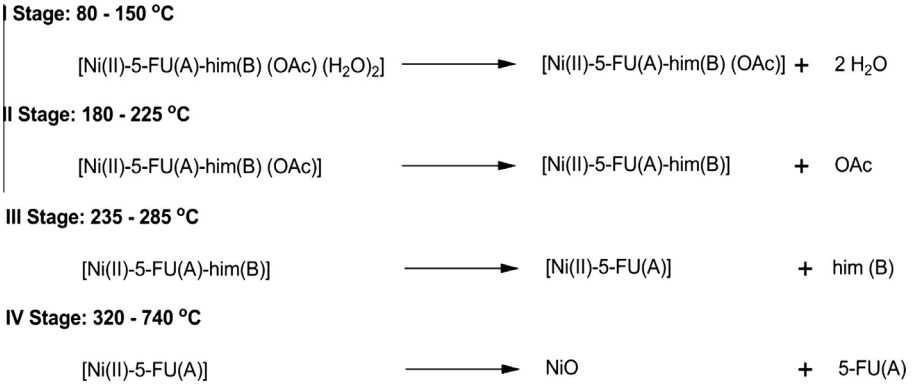

Scheme 2. Proposed thermogravimetric depiction of Ni(II)-5-FU(A)-him(B) complex (**3**).

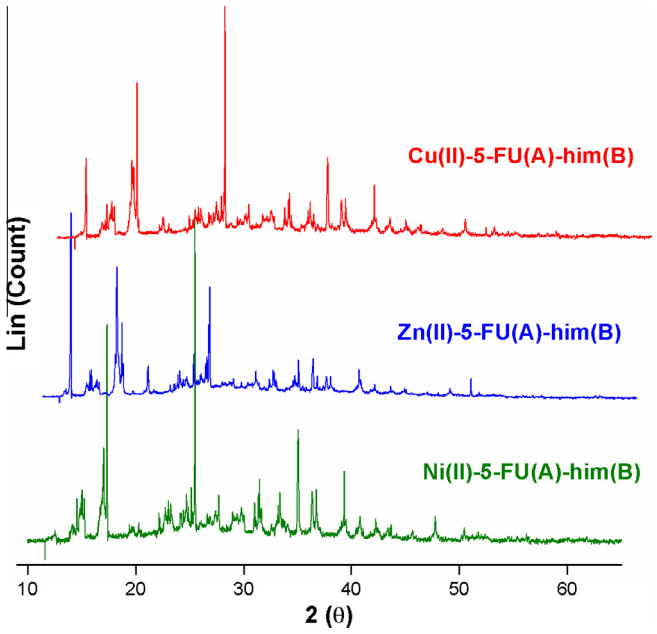

Fig. 4. X-ray diffraction patterns of M(II)-5-FU(A)-him(B) complexes **(1–3)**.

believe that the synthesized mixed ligand complexes have homogeneous phase material.

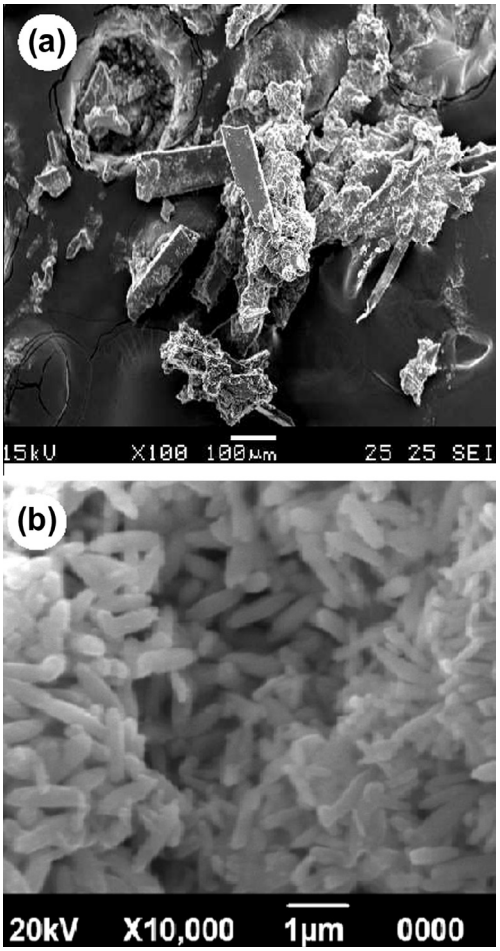

Fig. 5. SEM photographs of (a) Ni(II)-5-FU(A)-bim(B) complex (**4**) and (b) Cu(II)-5-FU(A)-bim(B) complex (**5**).

In vitro antimicrobial activity

In vitro antimicrobial activities of the free ligands *viz.*, of 5-Fluorouracil(A), imidazole(B), benzimidazole(B) and their M(II)-5-FU(A)-him/bim(B) complexes **(1–6)** were tested against five pathogenic bacteria and three fungal strains by well diffusion method using agar as nutrient (concentration of each complex = 30 µg in DMSO solution). Measured zone of inhibition (in mm) against the growth of bacterial and fungal for the above systems are given in Table S2 (Supplementary data file) and are shown in Fig. 6. The antimicrobial activity of the free ligands and their complexes are compared with the commercially available standard drugs, tetracycline (antibacterial control) and amphotricine (antifungal control). The antimicrobial activities of the mixed ligand complexes depend upon the size, charge distribution, shape and redox potential of the M(II) ions [48].

All the mixed ligand complexes show moderate activity than the corresponding free ligands against different types of microorganism. Variations in the effectiveness of different biocidal species

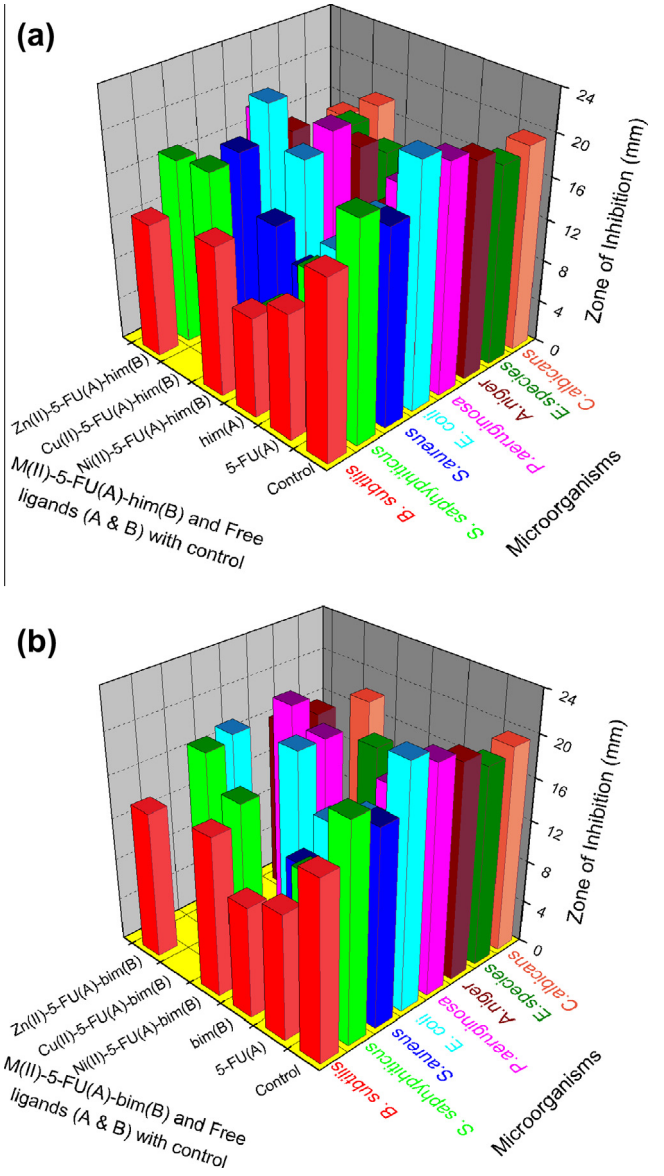

Fig. 6. Biological activities of (a) free ligands (A & B) & M(II)-5-FU(A)-him(B) complexes (**1–3**) and (b) free ligands (A & B) & M(II)-5-FU(A)-bim(B) complexes (**4–6**) with different microorganisms.

against microorganisms depend on the impermeability of the cell of the microbes or the changes in the nature of ribosomes of microbial cells [49]. Higher inhibition zones of mixed ligand complexes can be explained on the basis of Overtone's concept and Tweedy's chelation theory [50,51]. The significance of this work lies that, these mixed ligand complexes could be applied reasonably in healing of some common diseases like septicaemia, gastroenteritis, urinary tract illness and hospital acquired infections caused by Bacillus subtilis and Escherichia coli [52]. In addition, the distinctive possessions of the investigated mixed ligand complexes could be applied safe and sound in the treatment of infections caused by any of these particular strains. All the mixed ligand complexes show more significant antibacterial and less pronounced antifungal activities. This enhanced activities may be due to the presence of additional electron withdrawing [19,20] group present in 5-Fluorouracil (C_5—F) and also the imidazole moieties in them. The results clearly show that the order of antimicrobial activity, among the mixed ligand complexes, is Control > **(5)** > **(2)** > **(1)** > **(4)** > **(3)** > **(6).**

In vitro antioxidant activity

Antioxidant activities of 5-Fluorouracil(A) and its mixed ligand complexes Ni(II)/Cu(II)/Zn(II)-5-FU(A)-him/bim(B), (**1–6**) at 37 °C were studied *in vitro* by DPPH free radical scavenging methods. DPPH is a stable free radical that is often used for finding the radical scavenging activity in chemical analysis [53]. Ascorbic acid (AA) is used as the reference or positive control. All the analyses were done in three replicates and the results are averaged (Table 4).

Reduction capability of DPPH radical is determined by the decrease in its absorbance at 517 nm (blank) which can be induced by the antioxidant. From the results, it is seen that the mixed ligand complexes have higher activities than free ligands which may be due to the presence of the metal moiety and 5-Fluorouracil(A) which itself shows some activity [53].

Interaction of DNA with ligands and their mixed ligand complexes

DNA binding studies by electronic absorption method

Electronic absorption spectral technique is used to investigate the interaction of the complexes **(1–3)** with CT DNA. Electronic spectra of the Ni(II), Cu(II) and Zn(II)-5-FU(A)-him(B) complexes **(1–3)** in the absence and presence of CT DNA are shown in Fig. S3 (Supplementary data file). When the magnitude of CT DNA is increased, the absorption bands of the complexes are also affected (Table 5). The binding of the metal complexes to DNA through intercalation can be observed usually from the reduction in the intensity of the charge transfer bands to the extent of 5–15% along with the red shift (bathochromic shift). In general, a red shift is associated with the strong intercalative binding between the metal complexes and the base pairs of CT DNA helix [54].

The intrinsic binding constant (K_b) is determined from the plot of [DNA]/($\varepsilon_a - \varepsilon_f$) versus [DNA] from the absorption maxima in the range of 240–320 nm. The intrinsic binding constant for Ni(II)/Cu(II)/Zn(II)-5-FU(A)-him(B) complexes **(1–3)** are 3.215, 5.922 and 2.469 × 10^4 mol^{-1} respectively. From the observed values, it is clear that Cu(II)-5-FU(A)-him(B) complex **(2)** has significantly enhanced binding affinity when compared to Ni(II) and Zn(II) complexes. In addition, these binding constant values follow the order of stability. The higher binding constant value observed in the Cu(II) complex **(2)** may be due to its ability to counterbalance the dinegative charge of the phosphate sugar backbone of the DNA helix to some extent [55]. From the intrinsic binding constant (K_b), the free energy change ($\Delta^{\ddagger}G$) values are also calculated (Table 5) and these results indicate that the mixed ligand complexes can interact with the DNA in a spontaneous manner.

Oxidative DNA cleavage studies by gel electrophoresis method

Cleavage efficiency of the mixed ligand complexes with CT DNA is studied by gel electrophoresis method in the presence of an oxidant (H_2O_2). A representative cleavage pictograph of 5-Fluorouracil(A) and their mixed ligand complexes **(1–6)** are shown in Fig. S4 (Supplementary data file). The DNA cleavage efficiency of

Table 4
In vitro antioxidant activities of 5-Fluorouracil(A) and M(II)-5-FU(A)-him/bim(B) complexes (**1–6**) by DPPH free radical scavenging assay method at different concentrations (in μmol).

Complex	Scavenging activity (%)[a]				
	10 μmol	20 μmol	30 μmol	40 μmol	50 μmol
Ascorbic acid[b]	85 ± 0.17	88 ± 0.18	90 ± 0.20	92 ± 0.20	95 ± 0.21
5-Fluorouracil(A)	22 ± 0.25	26 ± 0.28	32 ± 0.27	34 ± 0.29	36 ± 0.33
Ni(II)-5-FU(A)-him(B)	36 ± 0.20	39 ± 0.26	41 ± 0.31	46 ± 0.37	51 ± 0.41
Cu(II)-5-FU(A)-him(B)	–	46 ± 0.30	50 ± 0.32	53 ± 0.34	58 ± 0.33
Zn(II)-5-FU(A)-him(B)	31 ± 0.19	35 ± 0.25	38 ± 0.36	42 ± 0.43	48 ± 0.42
Ni(II)-5-FU(A)-bim(B)	34 ± 0.24	37 ± 0.29	42 ± 0.32	44 ± 0.35	48 ± 0.39
Cu(II)-5-FU(A)-bim(B)	–	41 ± 0.41	49 ± 0.44	54 ± 0.46	57 ± 0.48
Zn(II)-5-FU(A)-bim(B)	–	28 ± 0.20	33 ± 0.34	37 ± 0.42	44 ± 0.49

[a] Standard deviation (average of three replicates) and "–" denotes less activity.
[b] Ascorbic acid is used as the standard control.

Table 5
Intrinsic binding constant (K_b) and free energy change ($\Delta^{\ddagger}G$) of mixed ligand M(II)-5-FU(A)-him(B) complexes with variation of CT DNA at 37 °C.

Complex	λ_{max} (nm)		Δλ (nm)	H (%) [a]	K_b[b] /mol^{-1}	($\Delta^{\ddagger}G$) (kJ mol^{-1})
	Free	Bound				
Ni(II)-5-FU(A)-him(B)	263	268	5	12.09	3.215 × 10^4	−86.29
Cu(II)-5-FU(A)-him(B)	260	267	7	18.41	5.922 × 10^4	−91.32
Zn(II)-5-FU(A)-him(B)	261	265	4	11.82	2.469 × 10^4	−84.10

[a] $H(\%) = \left[\frac{(A_{free} - A_{found})}{A_{free}}\right] \times 100\%$.
[b] K_b = Intrinsic DNA binding constant.

the M(II)-5-FU(A)-him/bim(B) complexes are due to the different extent of affinity of the complexes towards DNA. From the pictograph, it is shown that the nature of M(II) ions play an important role in the cleavage of isolated DNA. Control experiment using CT DNA alone (Lane C) does not show any significant cleavage even on longer exposure time. In general, the oxidative cleavage is proposed to account the cleavage of CT DNA caused by M(II) ions reacting with the co-reactant H_2O_2 to produce the molecular oxygen or peroxy derivatives or diffusible hydroxyl radicals via the abstraction of a hydrogen atom from sugar units (usually at C_4' position). This also predicts the release of specific residues arising from transformed sugars, depending on the position from which the hydrogen atom is removed and finally cleaves CT DNA [56]. Further, the reaction is modulated by a metallo complex bound to a peroxo species generated from the co-reactant H_2O_2, which may damage DNA through Fenton type chemistry [57]. The results from the pictograph shows that three out of seven systems including the free 5-FU(A) ligand have the ability to cleave the CT DNA in the presence of oxidant. In the present experiment, the mixed ligand complexes show a considerable extent of cleavage than the free ligand(A).

Conclusion

In the present study, mixed ligand complexes containing Ni(II)/Cu(II)/Zn(II) ions with the ligands 5-Fluorouracil(5-FU: A) and imidazole(him: B)/benzimidazole(bim: B) were synthesised and characterized by various spectral techniques. The spectral studies indicate that the ligand 5-FU(A) and him/bim(B) bind the M(II) ion via, the deprotonated $N_{(3)}$, $C_{(4)}$=O of 5-Fluorouracil and imidazole ring —$N_{(3)}$ atoms which form a stable metal chelates. The powder XRD and SEM analysis show that the mixed ligand complexes display sharp crystalline peaks with well-defined microcrystalline nature. The complexes show homogeneous particle nature with an average grain size of 57–66 nm. In the present investigation, Ni(II) complexes **(1 & 4)** show distorted octahedral environment whereas Cu(II)/Zn(II) complexes **(2, 3, 5 and 6)** show distorted tetrahedral geometry which are further supported by NMR and thermogravimetric analysis. The *in vitro* antimicrobial and antioxidant investigations show that the mixed ligand complexes have more potent activities than free ligands. Oxidative DNA cleaving activities of the mixed ligand complexes (except complexes **3 & 6**) with CT DNA under aerobic conditions show moderate activity in the presence of oxidant. Also, the absorption binding studies of CT DNA with the M(II)-5-FU(A)-him(B) complexes show a decrease in intensity of 5–15% with minor red shift values. The free energy change values ($\Delta^{\ddagger}G$) indicate the M(II) complexes can interact with DNA in a spontaneous manner.

Acknowledgements

All of us dedicate this paper to our beloved late Professors Dr. T.C. Manohar and K. Natesan, Department of Chemistry and Research Centre, South Travancore Hindu College, Nagercoil, India. PSM and SS thank the Management of Aditanar College of Arts and Science, Tiruchendur for providing Research facilities. We are grateful to STIC, CUSAT, Cochin for providing the analytical facilities.

Appendix A. Supplementary material

Supplementary data associated with this article can be found, in the online version, at http://dx.doi.org/10.1016/j.saa.2014.01.089.

References

[1] N.M. Goudgaon, N.J. Basha, S.B. Patil, Indian J. Pharm. Sci. 71 (6) (2009) 672–677.
[2] B.K. Karale, C.H. Gill, M. Khan, V.P. Chavan, A.S. Mane, M.S. Shingare, Indian J. Chem. 41B (9) (2002) 1957–1959.
[3] R.B. Patel, P.S. Desai, K.H. Chikhalia, Indian J. Chem. 45B (3) (2006) 773–778.
[4] A.E.E. Amr, N.M. Sabry, M.M. Abdulla, Monatsh. Chem. 138 (7) (2007) 699–707.
[5] E. Wagner, K. Al-Kadasi, M. Zimecki, W. Sawka-Dobrowolska, Eur. J. Med. Chem. 43 (11) (2008) 2498–2504.
[6] I.V. Ukrainets, I.A. Tugaibei, N.L. Bereznyakova, V.N. Kravchenko, A.V. Turov, Chem. Heterocycl. Compd. 44 (5) (2008) 565–575.
[7] W. Yang, Z. Ruan, Y. Wang, K. Van Kirk, Z. Ma, B.J. Arey, C.B. Cooper, R. Seethala, J.H. Feyen, J.K. Dickson, J. Med. Chem. 52 (4) (2009) 1204–1208.
[8] H.T.Y. Fahmy, S.A.F. Rostom, M.N. Saudi, J.K. Zjawiony, D.J. Robins, Arch. Pharm. Pharm. Med. Chem. 336 (3) (2003) 165–174.
[9] K. Hofmann, The Chemistry of Heterocyclic Compounds Imidazole and Its Derivatives, Part I, Interscience Publishers Inc., New York, 1953.
[10] C. Congiu, M.T. Cocco, V. Onnis, Bioorg. Med. Chem. Lett. 18 (3) (2008) 989–993.
[11] A.T. Mavrova, P. Denkova, Y.A. Tsenov, K.K. Anichina, D.I. Vutchev, Bioorg. Med. Chem. 15 (18) (2007) 6291–6297.
[12] S. Krupanidhi, A. Sreekumar, C.B. Sanjeevi, Indian J. Med. Res. 128 (2008) 448–461.
[13] F.H. Nielsen, Essentiality and function of nickel, in: W.G. Hoekstra, J.W. Suttie, H.E. Ganther, W. Mertz (Eds.), Trace Element Metabolism in Animals, second ed., University Park Press, Baltimore, 1974.
[14] P.J. Aggett, J.G. Comerford, Nutr. Rev. 53 (9) (1995) S16–S22.
[15] D.S. Sigman, A. Mazumder, D.M. Perrin, Chem. Rev. 93 (1993) 2295–2316.
[16] R. Pradhan, A.M. Thomas, A. Mukherjee, S. Dhar, M. Nethaji, A.R. Chakravarty, Indian J. Chem. 44A (2005) 18–26.
[17] P. Subbaraj, A. Ramu, N. Raman, J. Dharmaraja, Spectrochim. Acta 117A (2013) 65–71.
[18] J. Dharmaraja, T. Esakkidurai, P. Subbaraj, Sutha Shobana, Spectrochim. Acta 114A (2013) 607–621.
[19] S. Shobana, J. Dharmaraja, S. Selvaraj, Spectrochim. Acta 107A (2013) 117–132.
[20] S. Shobana, J. Dharmaraja, P. Kamatchi, S. Selvaraj, J. Chem. Pharm. Res. 4 (12) (2012) 4995–5004.
[21] M.A. Neelakantan, S.S. Mariappan, J. Dharmaraja, K. Muthukumaran, Acta Chim. Slov 57 (2010) 198–205.
[22] M.A. Neelakantan, F. Russal Raj, J. Dharmaraja, J. Johnsonraja, T. Jeyakumar, M. Sankaranarayana Pillai, Spectrochim. Acta 71A (2008) 1599–1609.
[23] M.A. Neelakantan, S.S. Marriappan, J. Dharmaraja, T. Jeyakumar, K. Muthukumaran, Spectrochim. Acta 71A (2008) 628–635.
[24] D.D. Perrin, W.L.F. Armarego, D.R. Perrin, Purification of Laboratory Chemicals, Pergamo Press, Oxford, 1980.
[25] A. Earnshaw, Introduction to Magneto Chemistry, Academic Press, New York, 1968.
[26] M.J. Pelczar, E.C.S. Chan, N.R. Krieg, Microbiology, fifth ed., Blackwell Science, New York, 1998.
[27] M.S. Blois, Nature 181 (1958) 1199–1200.
[28] A. Hussain, S. Saha, R. Majumdar, R.R. Dighe, A.R. Chakravarty, Indian J. Chem. 50A (3-4) (2011) 519–530.
[29] N.J. Farrer, L. Salassa, P.J. Sadler, Dalton Trans. (2009) 10690–10701.
[30] J. Marmur, J. Mol. Biol. 3 (2) (1961) 208–218.
[31] A. Wolfe, G.H. Shimer, T. Meehan, Biochemistry 26 (20) (1987) 6392–6396.
[32] W.J. Geary, Coord. Chem. Rev. 7 (1971) 81–122.
[33] K. Nakamoto, Infrared and Raman Spectra of Inorganic and Coordination Compounds, Wiley, New York, 1986.
[34] J.R. Ferraro, Low Frequency Vibrations of Inorganic and Coordination Compounds, Plenum Press, New York, 1971.
[35] G.C. Percy, D.A. Thornton, J. Inorg. Nucl. Chem. 35 (8) (1973) 2719–2726.
[36] A.B.P. Lever, Electronic Spectra of dN ions in Inorganic Electronic Spectroscopy, second ed., Elsevier, Amsterdam, The Netherlands, 1984.
[37] C.J. Ballhausen, Introduction to Ligand Field Theory, McGraw-Hill, New York, 1962.
[38] D. Sutton (Ed.), Electronic Spectra of Transition Metal Complexes: An Introductory Text, first ed., University of Michigan, McGraw-Hill, New York, 1968.
[39] W.W. Simons, The Sadtler Handbook of Proton NMR Spectra, Sadtler Research Laboratories, Philadelphia, Sadtlerk, 1978.
[40] B.R. McGarvey, Electron spin resonance of transition metal complexes, in: R.L. Carlin (Ed.), Transition Metal Chemistry, vol. 3, Marcel Dekker, New York, 1966.
[41] W.A. Alves, R.H.A. Santos, A. Paduan-Filho, C.C. Becerra, A.C. Borin, A.M.D.C. Ferreira, Inorg. Chim. Acta 357 (2004) 2269–2278.
[42] A.W. Addison, Spectroscopic and redox trends from model systems, in: K.D. Karlin, J.A. Zubieta (Eds.), Copper Coordination Chemistry: Biochemical and Inorganic Perspectives, Adenine Press, Guilderland, New York, 1983.
[43] B.J. Hathaway, D.E. Billing, Coord. Chem. Rev. 5 (1970) 143–207.
[44] R.S. Srivastava, Inorg. Chim. Acta 56 (1981) L65.
[45] M.E. Brown, Introduction to Thermal Analysis, Kluwer Academic Publisher, London, 2001.
[46] H.H. Horowitz, G. Metzger, Anal. Chem. 35 (10) (1963) 1464–1468.

[47] M.A. Estermann, W.I.F. David, in: W.I.F. David, K. Shankland, L.B. Mccusker, Ch. Baerlocher (Eds.), Structure Determination from Powder Diffraction Data (SDPD), Oxford Science Publications, New York, 2002.
[48] K. Reddy, Bioinorganic Chemistry, New Age International Pvt. Ltd., New Delhi, 2003.
[49] W.E. Levinson, E. Jawetz, Medical Microbiology and Immunology Examination and Board Review, sixth ed., Appleton and Lange, USA, 2000.
[50] Y. Anjaneyulu, R.P. Rao, Synth. React. Inorg. Met. – Org. Chem. 16 (2) (1986) 257–272.
[51] B.G. Tweedy, Phytopathology 55 (1964) 910–914.
[52] E. Jawetz, J.I. Melnick, E.A. Adelberg, Review of Medical Microbiology, fourteenth ed., Lange Medical Publications, Los Anglos, CA, 1980.
[53] S.B. Bukhari, S. Memon, M. Mahroof-Tahir, M.I. Bhanger, Spectrochimica Acta Part A 71 (5) (2009) 1901–1906.
[54] S.A. Tysoe, R.J. Morgan, A.D. Baker, T.C. Strekas, J. Phys. Chem. 97 (8) (1993) 1707–1711.
[55] S. Tabassum, C. Pettinari, J. Organomet. Chem. 691 (2006) 1761–1766.
[56] G. Prativel, M. Pitie, J. Bernadou, B. Meunier, Angew. Chem. Int. Ed. Eng. 30 (6) (1991) 702–704.
[57] A.Y. Louie, T.J. Meade, Chem. Rev. 99 (9) (1999) 2711–2734.